The 6th International Conference on
Structural Health Monitoring of Intelligent Infrastructure
Hong Kong | 9-11 December 2013

ADVANCES OF FIBER BRAGG GRATING SENSORS FOR STRUCTUR HEALTH MONITORING

H.N. Li, L. Ren and D.S. Li [1]
Dalian University of Technology, Dalian, Liaoning, China. Email: hnli@dlut.edu.cn

ABSTRACT

The past decade has seen rapid advances in research, development, and application of optical fiber Bragg grating technology. Sensors based on this technology have special advantages of being lightweight and small in size, inert and corrosion resistant, immune to electromagnetic interference (EMI), easily multiplexed and multifunctional (they can measure strain, temperature, pressure, and vibration) and these advantages made fiber Bragg grating sensors promising candidates for structural health monitoring. This paper serves as a tutorial to introduce the basics about fiber Bragg grating sensors, for structural health monitoring. The operating principles, strain transferring mechanism, types, the polytypic and synchronous data acquisition device and application example in the Dalian new gymnasium are presented in the paper. This paper will also review the-state-of-the-art of applications of fiber Bragg grating sensors for structural health monitoring.

KEYWORDS

Fiber bragg grating, structure health monitoring.

INTRODUCTION

A fiber Bragg grating (FBG) is a permanent periodic modulation of the refractive index in the core of a single mode optical fiber. The change of the core refraction index is between 10^{-3} and10^{-5}, and the length of a Bragg grating is usually around 10mm, which is much shorter than that of a long period grating (LPG) (De Vries 1998). This technology originated from the discovery of photosensitivity of Germanium doped Silica (Hill 1978). A more efficient transverse holographic method was devised (Meltz 1989), which enormously increased the scope of FBGs' applications. Now the phase mask technique supersedes the above two methods and is commonly used to commercially form the in-core gratings (Hill 1997). Techniques such as hydrogen loading and flame brushing can be adopted to enhance the germanium doped single mode optical fiber's photosensitivity prior to laser irradiation.

The principle of an FBG is described as follows. When light within a fiber impinges upon Bragg gratings, constructive interference between the forward wave and the contra-propagating light wave leads to narrowband back-reflection of light when the Bragg (or phase match) condition is satisfied. Because of this, a fiber Bragg gating can serve as an intrinsic sensor. Any local strain or temperature changes alter the index of core refraction and the grating period, followed by changes in wavelength of the reflected light. The wavelength changes can be detected by an interrogator, which employs edge filters, tunable narrowband filters, or CCD spectrometers (Kersey 1997; Rao 1997). Tunable narrowband filters are commercially popular interrogation systems. There are several major concerns in selecting FBGs and the associated interrogation systems. For instance, spectral overlap of the gratings changes adjacent desirable wavelength (Dakin and Volanthen 2000). For another instance, sidebands in the measured wavelength, the interrogation filter and the tunable light source also introduce errors to the system.
Fiber Bragg grating sensors could be particularly useful when the gratings with different periods are arranged along an optical fiber. Each of the reflected signals will have a unique wavelength and can be easily monitored, thus achieving multiplexing of the outputs of multiple sensors using a single fiber. Currently, up to 64 FBGs can be theoretically wavelength-multiplexed in one fiber, permitting quasi-distributive measurement of strain.
This paper introduces some principles of strain transferring of FBG sensors, which is the basis of FBG sensors application. Some packaged FBG sensors are presented in the paper, including strain sensor and temperature sensor. A polytypic and synchronous data acquisition device is introduced and this paper also reviews a typical application of FBG sensors for structural health monitoring in civil engineering.

STRAIN TRANSFERRING OF EMBEDDED FIBER BRAGG GRATING SENSORS

In the applications of fiber Bragg grating (FBG) sensors, the values measured by FBG sensors were assumed to be the actual structural strains (Baldwin 2001). In fact, they are not the same. The strains sensed by FBG sensors are different from actual host strains because of the difference between the modulus of the fiber and the modulus of the adhesive or the coating layer between the fiber and the host.

In our model, consider a single optical fiber of Young's modulus, Eg, radius, rg embedded in a host material, separated by a middle layer of Young's modulus, Ec , radius, rm and Poisson's ratio, μ,as illustrated in Figure 1. The host material, assumed to be infinitely in all directions, is subjected to uniform axial stress. L is the half gauge length of an optical fiber sensor, and 2L is the total length that the fiber is bonded to the host material through middle layer. τ(x,r) is the shear stress in the middle layer a distance r above a given x coordinate along the center of the fiber, τ(x,rg) is the shear stress at a given x coordinate along the fiber-middle layer interface. σg, σc and σm are the axial stress in the fiber, middle layer and the host material, respectively.

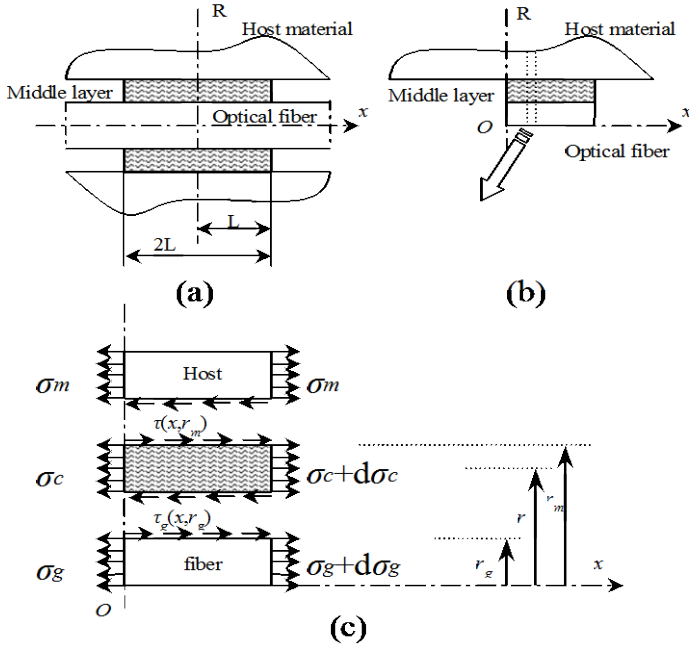

Figure 1. Coordinate system and free body diagram of symmetrical section of optical fiber: (a) Optical fiber of gauge length 2L; (b) One quarter of the fiber; (c) Stress distribution of the fiber and the coating

Based on stress equilibrium for a small segment of the fiber and the above assumptions, the longitudinal stress along the fiber σg, is related to the interfacial shear stress at the fiber/middle layer interface through,

$$\frac{d\sigma_g}{dx} = -\frac{2\tau(x,r_g)}{r_g} \tag{1}$$

thus, the final solution to (1), i.e. the strain distribution along fiber and its relationship to the strain of the host material at a given x coordinate is,

$$\varepsilon_g(x) = \varepsilon_m\left(1 - \frac{\cosh(kx)}{\cosh(kL)}\right) \tag{2}$$

(2) is the governing equation that describe the strain distribution along the fiber and its relationship to the strain of the host material at a given x coordinate. The effects on the strain transfer, of the Young's modulus of the fiber, the Young's modulus of the middle layer, and of the radiuses of the fiber and the middle layer, are all included in the strain lag parameter k defined in (3).

$$k^2 = \frac{2G_c}{r_g^{\,2} E_g \ln(\frac{r_m}{r_g})} = \frac{1}{(1+\mu)\frac{E_g}{E_c} r_g^{\,2} \ln(\frac{r_m}{r_g})} \tag{3}$$

Figure 2 shows the strain transfer rate along an optical fiber, and also the result by Ansari (Ansari &Yuan 1998) for comparison. The strain difference between the fiber and the host material at a given x coordinate, is determined by the strain lag parameter k. Figure 2 also demonstrates that the strain sensed by the fiber at the midpoint does not equals to the strain in the host material in this instance.

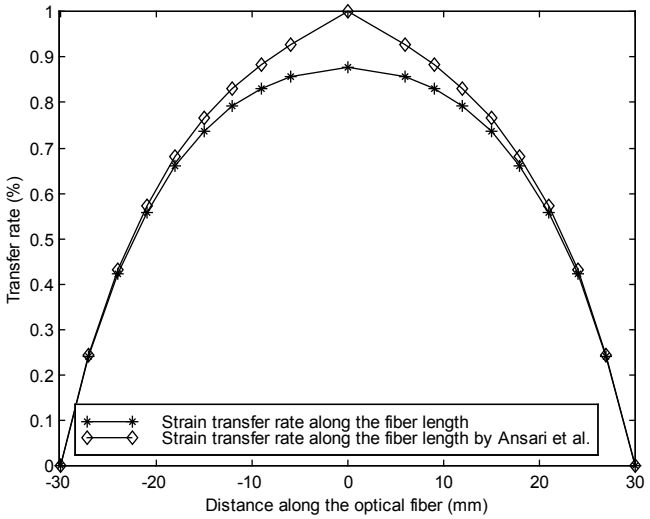

Figure 2. Distribution of normal strain in fiber along the length

FBG SENSORS

FBG Temperature Sensor

The Bragg wavelength shift is affected by temperature and strain that act on a specially treated section of FBG. Because quasi-distributed measurements can be easily realized by the use of wavelength division multiplexing technology, FBG sensors are suitable for applications in temperature measurement.

It is known that the wavelength shift is influenced by both strain and temperature. For a bare FBG without any packaging, the effect from strain, which is about 1.2 pm/με, is usually much higher than the effect from temperature which is about 10.8pm/℃ at λ_B =1520-1570nm. In the design of the FBG temperature sensor, several novel ways were put forward to reduce the adverse effect of strain availably and improve the thermal sensitivity remarkably. During the packaging process, the Bragg grating, protected with epoxide resin, is integrated into the stainless steel seamless thin-wall tube (Figure 3). Fiber Bragg gratings with wavelengths between 1525nm and 1565nm written into normal silica single-mode fibers are used.

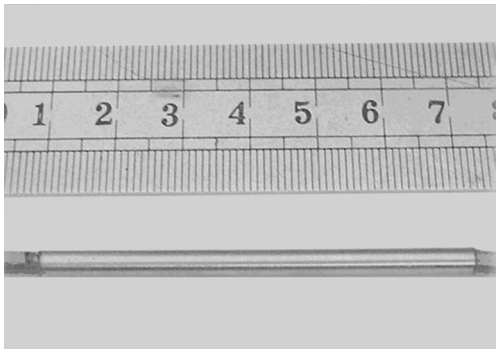

Figure 3. The picture of stainless steel tube-packaged FBG sensor

With being immersed in an epoxy resin, the fiber Bragg grating shows a different slope of its $\lambda_B(T)$ characteristics. It is approximately three times larger than theoretical value of a bare fiber Bragg grating, which is typically $\partial\lambda_B/\partial T$=10.8pm/℃ at λ_B=1520-1570nm. For the wavelength variations of the demodulating system ranging between ±2pm, the measurement accuracy of the tube-packaged FBG temperature sensor exceeds ±0.1℃.

FBG strain sensor

A FBG strain sensor (Figure 4), which is packaged by epoxy resin and stainless steel tube, is designed to measure the strain variation of structure. In the design of the FBG strain sensor, several novel ways were put forward to reduce the multi-peak effect of backreflecting wavelength, which is caused by non-uniform of epoxy resin.

The strain characteristics of sensor were studied by using universal material testing machine. An FBG strain sensor and a bare FBG were mounted directly on a steel plate and some strain gauges were placed close to the FBG sensor, then a tensile experiment was carried out using the steel plate. In the range of linear elasticity, the strain value was considered identically between FBG strain sensor, bare FBG and strain gauge.

Figure 4. The picture of stainless steel tube-packaged FBG strain sensor

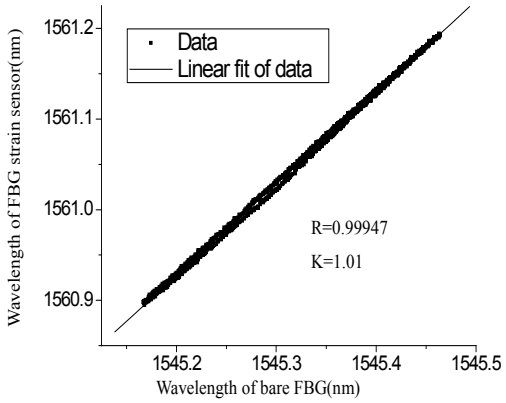

Figure 5. The wavelength variation relationship between of FBG strain sensor and bare FBG

In Figure 5, the steel plate is loaded continuously from 0 με to 250 με, then unloaded to 0με. It is shown that the linearity of the sensor's wavelength to bare FBG wavelength is very well, and the coefficient of linear association is more than 0.999 from Figure 10 and Figure 11. The packaging technique does not decrease the measurement accuracy of FBG, which is the same as the bare FBG.

POLYTYPIC AND SYNCHRONOUS DATA ACQUISITION DEVICE

In the field of structure health monitoring, more and more kinds of sensors have been applied to sense a number of physical measurement such as FBG for strain and electric sensors for acceleration, pressure, displacement, inclination and so on. A critical demand for a comprehensive data acquisition device to synchronously measure a great amount of polytypic sensors has been proposed to satisfy the requirements of data processing, calculation and structure analysis in some SHM projects.

A polytypic and synchronous data acquisition device system has been developed to measure the FBG sensors and electric signals, including voltage, current and digital I/O, which have covered most types of electric sensors. Figure 6 shows a schematic diagram of polytypic and synchronous data acquisition device.

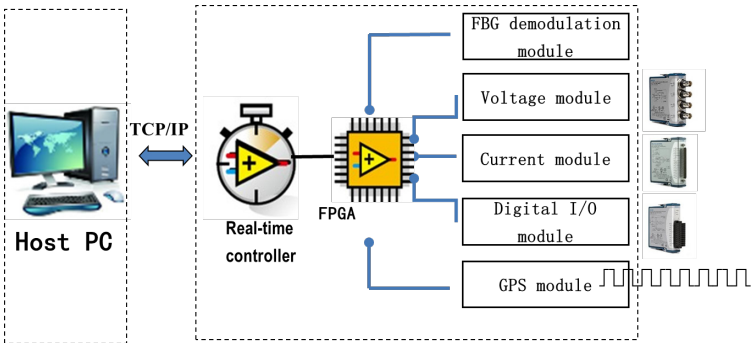

Figure 6. The schematic diagram of polytypic and synchronous data acquisition device

In this system, the signals from FBG and electric sensors passes through FBG demodulation module, voltage module, current module and digital I/O module respectively, which are controlled by FPGA (Field Programmable Gata Array). The FPGA acts as not only the analog signals input unit to sense both FBG and electric sensors but also the synchronous timer with 40MHz clock to trigger the signals sampling synchronously. The real-time controller contains an industrial processor that reliably and deterministically executes the data communication from the FPGA to host PC and offers multi-rate control for data acquisition.

Table 1 The specifications of polytypic and synchronous data acquisition device

	Sampling rate	Resolution	Protocol	Bandwidth	FBG Channels	Electric sensors channels
iFBG-S15	2Hz	1pm	TCP/IP	80nm	15	48

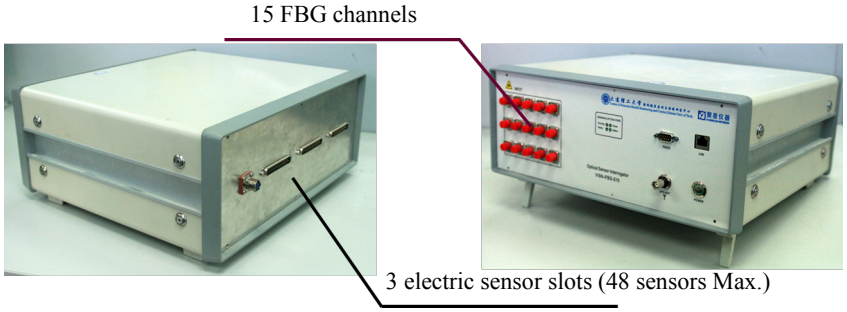

Figure 7. The polytypic and synchronous data acquisition device

This polytypic and synchronous data acquisition device was featured with the following characteristics: (1) a high-power, low-noise swept laser source for FBG demodulation, an embedded hardware and real-time operating system with industrial stability, a custom data communication protocol (DUT_SHM protocol), a synchronous data acquisition mechanism for polytypic signals.

DESIGN AND DEVELOPMENT OF STRUCTURAL HEALTH MONITORING SYSTEM FOR DALIAN NEW GYMNASIUM

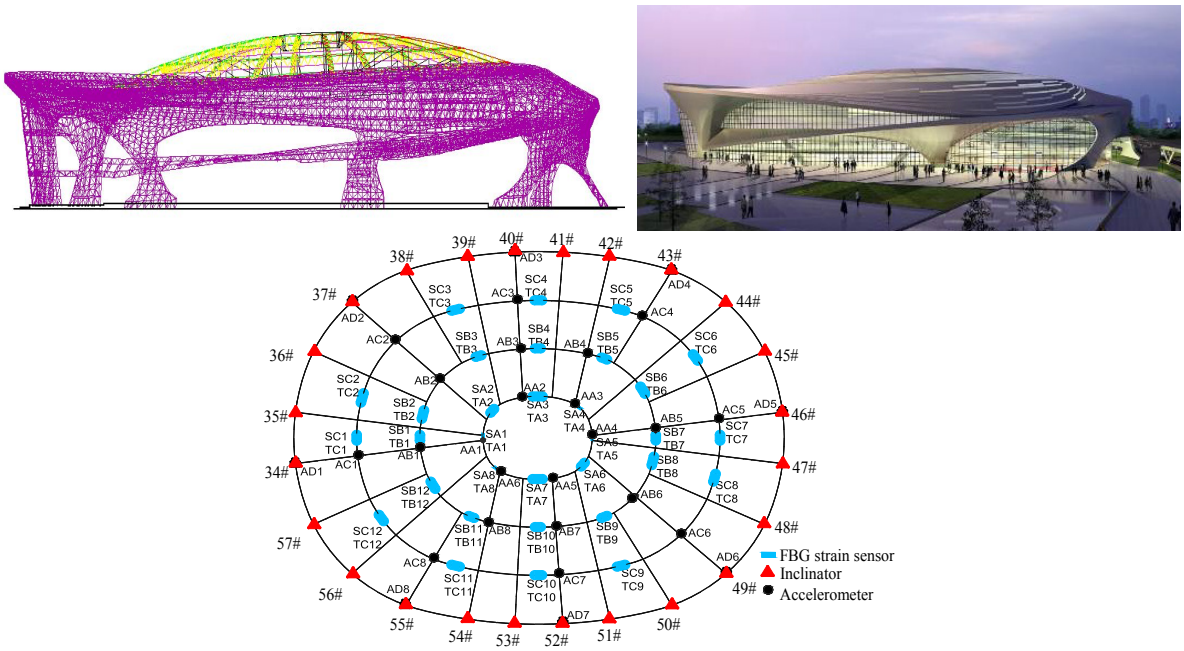

Figure 8. The CAD model of gymnasium structure and effect picture

The Dalian gymnasium consists of several different substructures. The main substructures consist of stands, building envelope and the roofing structure as it is shown in the Figure 8. The stands lying directly on the ground are made of reinforced concrete frame structure. It allows for 18,000 spectators. The roofing structure adopted suspend-reticular shell is supported by concrete column through 46 support abutments and its span is 145.4m. The lower boom consists of steel pulling cable system and is linked to top boom by 174 pulling cables. The building envelope adopts space frame structure. Figure 8 shows the sensors' location for structure health monitoring of this gymnasium.

Cable Force Monitoring

According to theoretical calculations, 24 representative cables adhered with FBG sensors on anchors were chosen as monitoring objects when the mega truss was in construction stage. They were equally installed on the three circles, presented in Figure 9, in which the dots denote the mounting positions of FBG sensors. Every cable has two anchors at its each end. The tension anchor is bolted with the lower end of the vertical struct, where oil jack is also installed to exert tension force, while the fixing anchor is directly bolted on the mega truss.

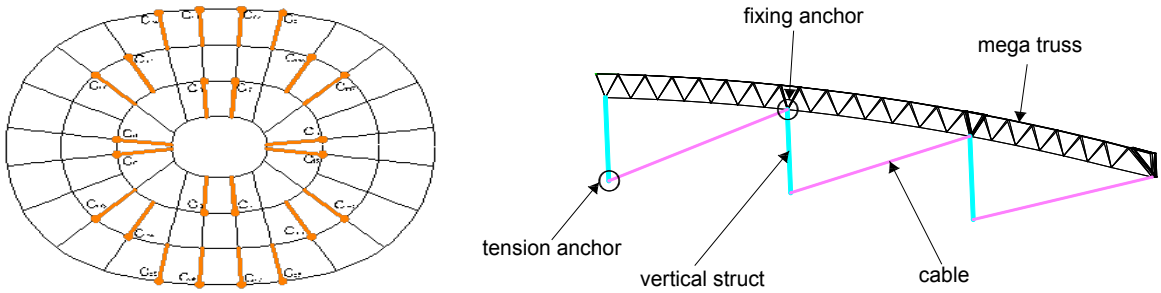

Figure 9. Sketch of FBG cable force sensor locations

The stretching process of cable Ci1 is presented in Figure 10. In prior to exert tension force, the oil jack is installed at the end of the cable which makes a portion of cable force transited from cable into the jack, resulting in an instant cable force decreasing. Afterwards, during the tensioning process, a tension increment is acquired and calculated by monitoring system. In this stretching step, an increment of approximate 270kN (from 80kN to 350kN) is read out based on FBG strain sensor calibration test on cable. However, a small fluctuation also exists in the acquired signal before and after the stretching process, which is caused by temperature variation.

Nevertheless, since the increasing slope is gentle, the tensioning process can be easily distinguished from the temperature influence, which thus can be neglected when process the signal.

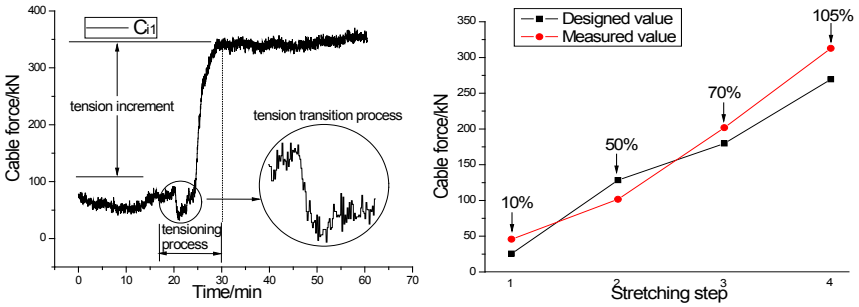

Figure 10. Time-history of cable stretching process and comparison result

After the whole stretching process, the cable force of each stretching step was verified by comparison with the designed cable force. Cable force comparison of designed and measured value of Ci1 is presented in Figure 7, from which an average error rate less than 20% was calculated. In consideration of thermal expansion and contracting of steel anchor caused by temperature influence, this error rate is acceptable. Since it's a short-term process, temperature has little influence on real-time monitoring of stretching construction. However, the temperature effect cannot be neglected when analyzing long-term data. The ambiguousness of temperature effect still needs to be investigated.

Site Blasting Monitoring

A structural dynamic response, shown in Figure 11, was detected and stored by the monitoring system when the site blasting was carrying out near the gymnasium. Based on signal transferring theory and Fast Fourier Transform (FFT) algorithm, structural modal parameters were identified. The calculating fundamental frequency of the mega truss is 2.45 HZ.

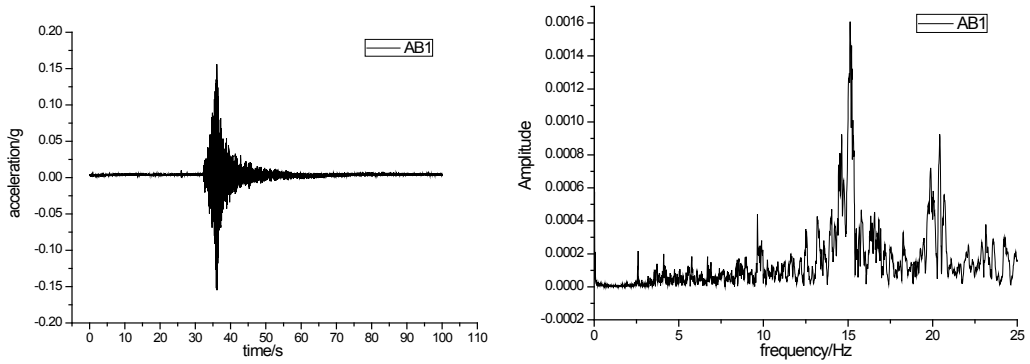

Figure 11. Time-history of structural dynamic response and acceleration frequency spectrum

CONCLUSIONS

This paper presents a review of resent research and development activities in structural health monitoring of civil structures using Fiber Bragg Grating (FBG). Although the progress of fiber optic health monitoring is impressive, it is yet to reach its full potential especially in terms of the market exploitation. One of the exciting fields wherein fiber optic sensors and health monitoring is expected to play a significant role is smart structures and intelligent systems. In smart structure applications, composite materials, fiber optic sensing systems, piezoelectric actuators and microprocessor based control schemes seem to offer the best advantages in the future.

REFERENCES

Ansari, F. and Libo, Y. (1998). "Mechanics of bond and interface shear transfer in optical fiber sensors", *J. Engrg. Mech.*, ASCE, 124(4), 385-394.

Baldwin, C.S., Poloso, T., Chen, P.C., Niemczuk, J.B., Kiddy, J.S. and Ealy, C. (2001). “Structural monitoring of composite marine piles using optical fiber sensors”, Proc., SPIE, *Smart Structures and Materials and Nondestructive Evaluation for Health Monitoring and Diagnostics*, 4330, 487-497.

Dakin, J.P. and Volanthen, M. (2000). “Distributed and multiplexed fiber grating sensors, including discussion of problem areas”, *IEICE trans. Electron,* E83-C (3), 391-399.

De Vries, M., Bhatia, V., D'Alberto, T., Arya, V. and Claus, R.O. (1998). “Photo induced grating-based optical fiber sensors for structural analysis and control”, *Engineering structures*, 20(3), 205-210.

Hill, K.O., Fujii, Y., Johnson, D.C. and Kawasaki, B.S. (1978). “Photosensitivity in optical fiber waveguides: application to reflection fiber fabrication”, *Appl. Phys. Lett,* 32, 647-650.

Kersey, A.D., Davis, M.A., Patrick, H.J., LeBlanc, M., Koo, K.P., Askins, C.G., Putnam, M.A. and Friebele, E.J. (1997). “Fiber grating sensors”. *Journal of lightwave technology* 15(8), 1442-1463.

Meltz, G., Morey, W.W. and Glenn, W.H. (1989). “Formation of Bragg gratings in optical fibers by a transverse holographic method”, *Optics Letters,* 14(15), 823-825.

Rao, Y.J. (1997). “In-fiber Bragg grating sensors”, *Measurement Science and Technology*, 8, 355-375.